The Journal of Experimental Biology 212, 3349-3360
Published by The Company of Biologists 2009
doi:10.1242/jeb.033639

Mono- *versus* biarticular muscle function in relation to speed and gait changes: *in vivo* analysis of the goat triceps brachii

Andrew M. Carroll[1,*] and Andrew A. Biewener[2]

[1]Department of Biology, University of Evansville, 1800 Lincoln Avenue, Evansville, IN 47722, USA and [2]Concord Field Station, Harvard University, 100 Old Causeway Road, Bedford, MA 01730, USA

*Author for correspondence (ac204@evansville.edu)

Accepted 16 July 2009

SUMMARY

The roles of muscles that span a single joint (monoarticular) *versus* those that span two (biarticular) or more joints have been suggested to differ. Monoarticular muscles are argued to perform work at a joint, whereas biarticular muscles are argued to transfer energy while resisting moments across adjacent joints. To test these predictions, *in vivo* patterns of muscle activation, strain, and strain rate were compared using electromyography and sonomicrometry in two major elbow extensors, the long and lateral heads of the triceps brachii of goats (*Capra hircus*), across a range of speed (1–5 m s^{-1}) and gait. Muscle recordings were synchronized to limb kinematics using high-speed digital video imaging (250 Hz). Measurements obtained from four goats (25–45 kg) showed that the monoarticular lateral head exhibited a stretch-shortening pattern (6.8±0.6% stretch and –10.6±2.7% shortening; mean ± s.e.m. for all speeds and gaits) after being activated, which parallels the flexion–extension pattern of the elbow. By contrast, the biarticular long head shortened through most of stance (–16.4±3.4%), despite elbow flexion in the first half and shoulder extension in the last half of stance. The magnitude of elbow flexion and shoulder extension increased with increasing speed (ANCOVA, $P<0.05$ and $P<0.001$), as did the magnitude and rate of active stretch of fascicles in the lateral head ($P<0.001$ for both). In all individuals, shortening fascicle strain rates increased with speed in the long head ($P<0.001$), and, in three of the four individuals, strain magnitude increased. Few independent effects of gait were found. In contrast to its expected function, the biarticular long head appears to produce positive work throughout stance, whereas the monoarticular lateral head appears to absorb work at the elbow. The biarticular anatomy of the long head may mitigate increases in muscle strain with speed in this muscle, because strain magnitude in the second phase of stance (when the shoulder extends) decreased with speed ($P<0.05$).

Supplementary material available online at http://jeb.biologists.org/cgi/content/full/212/20/3349/DC1

Key words: muscle function, biarticular, fascicle strain, electromyography (EMG), *Capra hircus*, kinematics, triceps.

INTRODUCTION

Muscle–tendon units (MTUs) in animal limbs can be categorized as monoarticular if they cross one joint, biarticular if they cross two joints, and multiarticular if they cross three or more joints. Monoarticular muscle tendon units must lengthen or shorten with the flexion or extension of the joint they cross. If monoarticular MTUs contain relatively long tendons, lengthening and shortening may largely occur in series-elastic passive structures allowing muscle fascicles to contract isometrically. For muscles that lack long tendons, such as many proximal limb muscles, lengthening and shortening must be taken up by muscle fascicles. For instance, the vastus lateralis (VL) of many species appears to stretch and shorten with flexion and extension of the knee (e.g. Gillis and Biewener, 2001). For bi- or multiarticular proximal MTUs, flexion or extension at one joint may be offset by motion at adjacent joints, allowing the muscle to contract isometrically (Kaya et al., 2005), and thus more economically (Roberts et al., 1997; Biewener and Roberts, 2000). This enables the MTU to contribute simultaneous moments at both joints (van Igen Schenau, 1990), while providing transfer of energy from one joint to another (Cleland, 1867; Prilutsky and Zatsiorsky, 1994).

The prevalence of the ‘strut-like’ function in the literature (van Igen Schenau, 1990; Jacobs et al., 1993; Gorb and Fischer, 2000; Witte et al., 2002) may overshadow a separate, though not mutually exclusive, role for biarticular muscles in work production through active fascicle shortening. In particular, there may be situations in which anatomical factors suggest an alternative function for shortening and work production. A relatively large, long-fibered condition in a multiarticular muscle may reflect a functional requirement for fascicle shortening and work production, rather than strut-like isometric force production (Payne et al., 2005a; Payne et al., 2005b). Additionally, if a multiarticular muscle is more massive than those proximal to it, it would not make sense for it to transfer energy from smaller muscles without performing work itself.

The long head of the triceps brachii (Tr_{LONG}) is a flexor at the shoulder joint (i.e. it rotates the humerus caudally in the sagittal plane; Fig. 1). Consequently, it is able to transfer energy from shoulder extension to elbow extension in the manner consistent with the strut-like function described above. However, morphological properties of the Tr_{LONG} suggest a role in work production less commonly ascribed to biarticular muscles. First, it is relatively long fibered (Payne et al., 2005b), an architecture associated with work or displacement producing muscles (Lieber, 2002). Second, it is massive relative to other intrinsic and extrinsic forelimb musculature (Payne et al., 2005b; Williams et al., 2008). Although the mechanics of force balance and transmission in the forelimb are quite complex (English, 1978), the combined mass of other muscle directly capable of extending the scapulo-humeral joint (and thus, transferring

energy distally through the Tr_{LONG}), such as the biceps brachii or supraspinatus, is lower than that of the Tr_{LONG} in dogs (Williams et al., 2008) and horses (Payne et al., 2005b). Thus, the architecture and mass of this muscle suggests that it might be expected to shorten and contribute work to locomotion.

Published direct data on Tr_{LONG} function are inconsistent. Goslow et al. (Goslow et al., 1981) reported a continuous shortening pattern in the Tr_{LONG} throughout stance in dogs, based on limb kinematics. Direct measurements of Tr_{LONG} fascicle length change from sonomicrometry in running dogs (Gregersen et al., 1998) show an isometric pattern in the late stages of stance consistent with energy transfer but show brief shortening in early stance when energy transfer would be impossible because the shoulder and elbow are both flexing. By contrast, Witte et al. (Witte et al., 2002) (and references therein) assume an isometric role for the Tr_{LONG} in the early phase of stance in small mammals.

We measured aspects of *in vivo* muscle function including activation, strain, and strain rate in the Tr_{LONG} of goats (*Capra hircus* Linnaeus 1758) to broaden understanding of the functional repertoires of biarticular muscles. The functional role of the Tr_{LONG} was also compared with its monoarticular agonist, the lateral head of the triceps (Tr_{LAT}; Fig. 1). Based on a previous comparison of both muscles during jumping (Carroll et al., 2008), we predicted that the Tr_{LAT} would exhibit a stretch shortening pattern in parallel with the flexion and extension of the elbow, whereas the Tr_{LONG} would shorten throughout stance in a pattern similar to that predicted by Goslow et al. (Goslow et al., 1981) for running dogs.

Changes in muscle force, work, and mechanical power associated with changes in speed that are produced by the musculoskeletal system are linked to the energy cost of locomotion (or rate of oxygen uptake; $\dot{V}_{O_2}$) (e.g. Marsh and Ellerby, 2006; Taylor, 1994). Morphological factors that reduce the effects of increased locomotor speed on muscle force and work output can help to reduce the energy cost of increased locomotor speed for the animal and thus may increase sustainable speeds obtainable for a given $\dot{V}_{O_2,max}$. For example, increases in speed in hopping wallabies (*Macropus eugenii)* occur without concurrent increases in oxygen consumption, in large part, because long leg tendons store and return elastic energy, reducing the increase in muscle strain and work output that would otherwise be required at faster hopping speeds (Biewener et al., 1998). The ability to store and recover elastic energy from tendons allows the distal biarticular and multiarticular wallaby leg muscles to operate under nearly isometric conditions, favoring more economical force generation.

A second goal of the current study, therefore, was to understand how function of the long and lateral heads of the goat triceps varies with locomotor speed. We predicted that increases in locomotor speed would increase the magnitude and rate of stretch in the Tr_{LAT} due to increased loading in early stance, given that a similar pattern was found in the monoarticular vastus lateralis (VL) of goats and rats (Gillis et al., 2005; Gillis and Biewener, 2001). We also predicted that the biarticular arrangement of the Tr_{LONG} might mitigate changes in strain and strain rate associated with increases in speed, similar to the distal leg muscles of hopping wallabies described above (Biewener et al., 1998) and running turkeys (Roberts et al., 1997). In particular, increases in shoulder extension with speed may offset elbow extension to limit increases in strain and strain rate that would otherwise be required. In general, our hypothesis is that the biarticular arrangement of muscles represents a key morphological feature that contributes to a reduction in the cost of locomotion by reducing the effect of increased locomotor speed on muscle strain and strain rate.

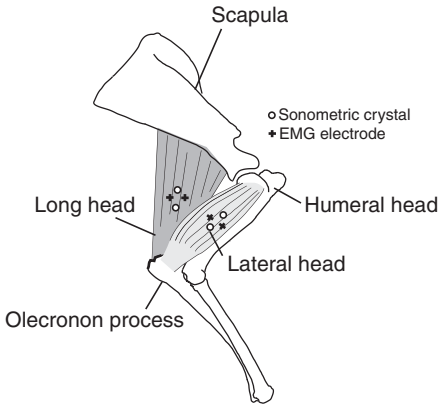

Fig. 1. General anatomy of the long (Tr_{LONG}) and lateral (Tr_{LAT}) heads of the triceps brachii of the forelimb of goats. Also shown are the approximate locations of sonomicrometric crystals and EMG electrodes used to measure muscle function. See the text for a more detailed description of the anatomy and methods.

MATERIALS AND METHODS

Animals

Methods and surgical procedures for this study were similar to those described by Carroll et al. (Carroll et al., 2008) and are briefly described here. Four goats (24, 27, 42 and 45 kg) were used in the study. An additional 15 kg goat was used in a separate x-ray cine analysis. Animals were housed outdoors in fields at the Concord Field Station, Bedford, MA, USA, and experiments conducted in accordance with Harvard IACUC guidelines and USDA regulations. Over a period of 2 to 3 weeks goats were trained to walk, trot, and gallop on a treadmill (belt: 2.5 m long and 0.75 m wide). During data collection an effort was made to record similar speeds (usually at 0.5 m s^{-1} increments) across animals; however, we also sought to elicit the fastest or slowest speed at which an animal would perform a certain gait. Thus, minimum and maximum speeds within a gait differed among some individuals. Values are reported as means ± s.e.m., unless otherwise noted.

Anatomy

The long head (Tr_{LONG}) and the lateral head (Tr_{LAT}) of the triceps both insert on the olecranon process of the ulna (Fig. 1). A much smaller (<5% mass of combined Tr_{LONG} and Tr_{LAT}) monoarticular medial head is also present but was not measured. The lateral head originates from the humerus, whereas the long head originates from the distal-most third of the ventro-caudal margin of the scapula. Consequently, the Tr_{LAT} is monoarticular and the Tr_{LONG} is biarticular. Architecturally, the Tr_{LAT} contains parallel fascicles that run the extent of its length (ranging from an average of 6.0±2 cm in a 25 kg goat to 8.0±3 cm, in a 45 kg goat). The Tr_{LONG} contains long fascicles of similar length (average: 6.5±3 cm in a 25 kg goat to 8.0±3 cm in a 45 kg goat), but is slightly unipinnate (15±4 deg.).

Surgery

Before surgery, animals were starved for 1 day. Goats were induced for intubation with 8 mg kg^{-1} ketamine and 0.5 mg kg^{-1} xylazine administered into the jugular vein. After intubation, goats were maintained in a surgical plane of anesthesia with 2–4% isoflurane by volume, administered *via* inspired oxygen. Sonomicrometric crystals (2 mm; Sonometrics Inc., London, ON, Canada) and bipolar

Table 1. Summary of ANCOVAs used in this study and referred to in the text

Test	Independent variables (d.f.)	Test data (number of observations)	Model d.f.	Error d.f.	Purpose of test
ANCOVA (Type I sequential SOS)	Speed (covariate, 1) Gait (2)	Individual means (33–34, per period and muscle)	3	29–30	Evaluate the effects of speed and gait within each muscle and period (yield, propulsive, stance) (Tables 2 and 3)
ANCOVA (Type III)	Speed (covariate, 1) Individual (3) Individual×speed (3)	Full data set (32–103 per individual) (210–308 total)	7	202–300	Evaluate effect of individuals on parameters and trends within each muscle head and period
ANCOVA (Type III)	Speed (covariate, 1) Muscle head (1)	Individual means (65–67 per individual)	2	62–64	Compare muscle heads within each period
ANCOVA (Type I sequential SOS)	Speed (covariate, 1)	Full data (within individuals) (32–103 per individual, muscle and period)	1	30–101	Evaluate the effects of speed and gait within each individual, muscle and period

electromyography (EMG) electrodes were fashioned from twisted strands of 0.102 mm enamel-coated silver wire (California Fine Wire Inc., Grover Beach, CA, USA) with a 3–4 mm dipole distance (Loeb and Gans, 1986). Care was taken to insert each pair of crystals along the fascicle axis 10–14 mm apart. In the long head, this meant implanting the distal crystal slightly deeper than the proximal because of the muscle's slight fascicle pinnation. EMG electrodes were inserted immediately lateral to those fascicles containing crystals using an 18.5 gauge hypodermic needle and were secured to the fascicles with 4-0 silk suture. The electrode connectors were then sutured to the skin of the neck with sterile 0 surgical wire. Goats were allowed to recover overnight. Data collection took place within 1 to 2 days after surgery. All animals were killed following data collection, with 120 mg kg^{-1} of commercial pentobarbital solution injected into the jugular vein.

Joint kinematics

The hoof and the skin overlying the metacarpophalangeal, wrist, and shoulder joints, and the scapular spine (at its most proximal palpable extent) were marked with non-toxic white paint. Kinematics were digitally recorded at 250 Hz using a Redlake PCI-500 video system (Redlake, Morgan Hill, CA, USA). Joint locations were digitized using a custom auto-tracking digitization program in MatLab (v. 6.5; The MathWorks, Natick, MA, USA) written by T. L. Hedrick, UNC, Chapel Hill, NC, USA (http://www.unc.edu/~thedrick/software1.html). Digitized data were filtered at 30 Hz with a fourth-order recursive (zero-lag) Butterworth filter, and used to determine hoof position, limb segment position, and elbow and shoulder angles for each sequence. The camera was controlled by an analog trigger, and the voltage signal from this trigger was used to synchronize camera recordings with EMG and sonomicrometry recordings. Shoulder flexion was defined with respect to the caudal (posterior) angle formed between the humerus and scapula in the sagittal plane (Fig. 1).

X-ray video kinematics were captured from a lateral X-ray video, recorded at 125 Hz, of a 15 kg goat walking and trotting on a motorized treadmill (0.7 m×1.20 m) at 0.9 and 2.5 m s^{-1}, respectively. A smaller goat was required for X-ray recordings, in order to fit the scapula, humerus and olecranon on the 30.5 cm diameter fluoroscopic screen for a full stride. Videos were recorded at 125 Hz with a high-speed Photron Fastcam camera (Photron, San Diego, CA, USA) mounted on the fluoroscope of the X-ray C-arm (Model 9400 C-Arms International, Hamburg, PA, USA). Raw video was corrected for fluoroscope distortion using a custom MatLab script available from David Baier (Department of Ecology and Evolution, Brown University; David_Baier@Brown.edu), and digitized as described above, except that the humeral angle had to be estimated from the position of the glenoid surface of the humerus. Position data were filtered with a low-pass filter at 15 Hz. Because the foot could not be seen in the X-ray video, the relative excursion of the elbow joint was used to estimate periods of stance and swing.

EMG

EMG signals were filtered (60 Hz notch and 30–3000 Hz bandpass) and amplified at 1000× with Grass P511 amplifiers (Grass-Telefactor, West Warwick, RI, USA). Outputs from the Grass amplifiers were digitized at 2000 Hz through a 12-bit A/D converter (Digidata 1200B, Axon Instruments, Union City, CA, USA). EMG signals were later digitally filtered (in MatLab) with a custom 100–1000 Hz bandpass fourth-order zero-lag Butterworth filter, prior to analysis.

Muscle strain

Sonomicrometric crystals measure latency of ultrasound transmitted between a pair of crystals to determine instantaneous muscle length. The speed of sound in muscle was estimated to be 1550 m s^{-1} (Mol and Breddels, 1982). Latency of crystal response was transduced and amplified with a Triton sonomicrometrics system (Model 120-1001; Triton Technology, San Diego, CA, USA) and digitized with the EMG signals at 2000 Hz as described above. Because sound propagation through the epoxy of the Sonometrics^{TM} crystals exceeds that through the muscle, an offset of +0.82 mm was applied to recordings made using the 2.0 mm crystals (Gillis et al., 2005). Owing to its filtering circuitry, there is also a 5 ms delay inherent in the Triton system that was accounted for in subsequent data analysis. Crystal distances were normalized to fascicle resting length measured during quiet stance to estimate fascicle strain.

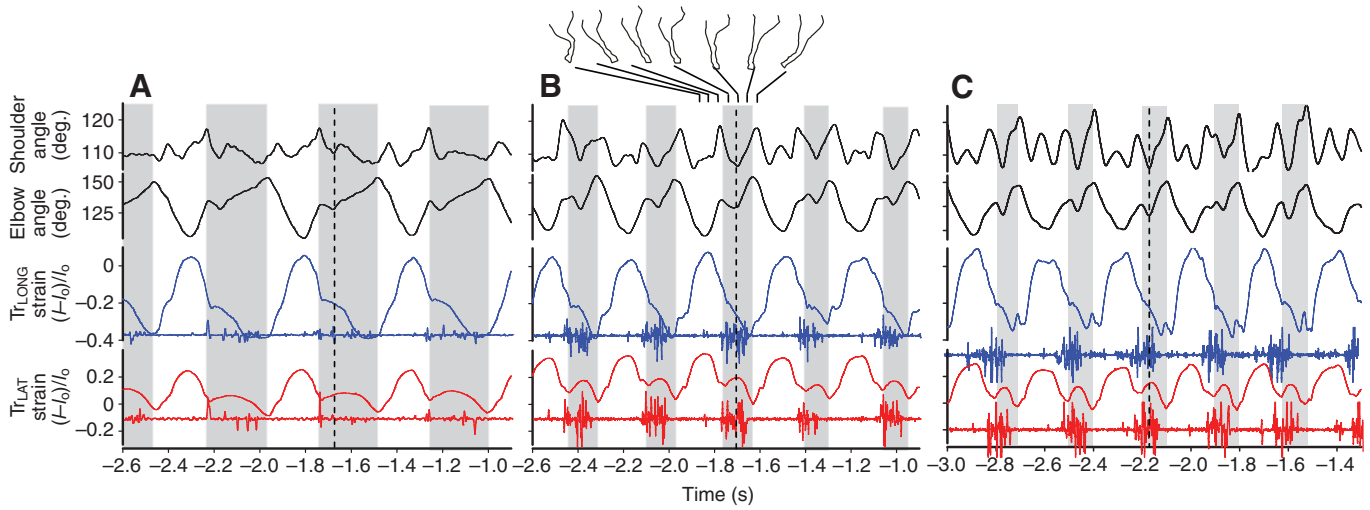

Fig. 2. Representative kinematic, strain and activation data from (A) a 1.5 m s^{-1} walk, (B) a 3 m s^{-1} trot and C. a 4.3 m s^{-1} gallop in a 24 kg goat. Elbow and shoulder joint angles are given in the top traces, fascicle strains and EMG are below (Tr_{LONG}, blue; Tr_{LAT}, red). Stance periods are indicated by grey shading. There was considerable within-individual variation even during steady running. Both the shoulder and elbow flexed at the onset of stance; in walking the shoulder remained flex, but in trotting and galloping it re-extended in the latter phase of stance. The elbow always flexed and extended; the dashed line indicates the transition from flexion to extension which was used to define 'yield' and 'propulsive' phases of stance. The long head shortened throughout most of stance whereas the lateral head showed a pattern of stretch and shortening that paralleled the flexion–extension pattern of the elbow.

Data analysis

Between three and seven steady strides were analyzed at each speed depending on the animal's running consistency at each speed. Occasionally no usable strides were available for a given individual at certain speeds (Figs 4–6 missing data at some speeds) because of unsteady locomotion at that speed or poor signal quality for some strides. Kinematics, muscle strain and strain rate were partitioned, measured and compared over defined periods of stance (as described below). EMG parameters however were not partitioned into periods of stance. EMG timing data were measured relative to foot-on at the start of stance in absolute terms and as percentages of stance time. Duty factor was also normalized to stance time. Rectified EMG intensity (mV) was normalized by the largest recorded value for each electrode over all trials of individual animals.

Various statistical analyses (see Table 1) were performed to compare the muscle heads and to assess the independent effects of gait and speed on limb joint kinematics and muscle function. To avoid pseudo-replication, tests were either conducted within individuals or on individual means when comparisons were made over a range of speeds. In all tests, speed was included as a covariate. Tests of speed and gait effects were compared using a sequential (Type 1) ANCOVA. Thus, if gait provided no explanatory power (i.e. non-significant *P*-value) after speed had been included in the analysis, it was considered to have no effect on the parameter. For comparisons between muscles or gaits, the least-squares means of each parameter were compared using *post-hoc* tests (Tukey's HSD) on least-squares means (mean values after the effect of speed had been removed). All tests were performed in JMP (SAS Institute, Cary, NC, USA)

RESULTS

Kinematics

Goats showed no evidence of lameness and moved normally on the treadmill following surgery. Stance time decreased with increasing speed ($P<0.001$) in a pattern closely resembling that described previously for the hind limb of goats (Gillis et al., 2005). Goats of the size used in this study transitioned from walking to trotting at speeds above 1.5 m s^{-1} and from trotting to galloping at 4–4.5 m s^{-1}, depending on size. Regardless of speed or gait, the elbow flexed at foot contact and re-extended before foot-off, resulting in net elbow extension (Fig. 2). Periods of elbow flexion and extension during stance were used to define the 'yield' and 'propulsive' phases (Phillipson, 1905) in subsequent analyses. As speed increased, there were weak trends towards increased flexion during the yield phase ($P<0.05$) and extension during propulsive phase ($P<0.05$; Fig. 4). These trends offset one another such that there was no change in net elbow angular excursion over stance phase ($P>0.50$; Fig. 4). Nor were there detectable independent effects of gait on elbow kinematics (Table 2).

During trotting and galloping, the shoulder underwent a parallel and simultaneous flexion and extension patterns to that observed in the elbow (Fig. 2). Yield phase flexion of the shoulder ($P<0.01$), as well as extension ($P<0.001$), increased with speed in a consistent pattern among individuals (Fig. 4B). Unlike the elbow, shoulder extension outpaced flexion resulting in increased net extension over stance with speed ($P<0.001$) and a longer effective step length ($P<0.05$).

The pattern described above was based on external kinematic markers, but X-ray video recording of a single 15 kg goat showed a similar flexion–extension pattern during trotting (Fig. 3). Both techniques showed flexion at the onset of stance during walking, but a brief period of shoulder extension appears in external kinematics that was not found using X-ray video recording (Fig. 3). Overall, shoulder extension during the propulsive phase appears to be reduced relative to that predicted by speed alone (Table 2, significant effect of gait during propulsive phase).

Muscle strain

Strain patterns in the Tr_{LAT} closely followed elbow kinematics, lengthening as the elbow flexed and shortening as it extended (Fig. 2). This resulted in net shortening in most individuals over all speeds and gaits (Fig. 5). By contrast, the Tr_{LONG} shortened

Table 2. *P*-values and trends from sequential (Type 1) ANOVA (d.f. in Table 1) results for speed and gait

	Yield				Propulsive				Stance			
	Speed		Gait		Speed		Gait		Speed		Gait	
	P value	Trend	*P* value	Trend	*P* value	Trend	*P* value	Trend	*P* value	Trend	*P* value	Trend
Tr_{LONG}												
Strain	<0.0001*	Increasing shortening	<0.01*	Trot>walk, gallop (strain magnitude)	<0.001*	Decreased shortening	0.73		0.98†	N/A	0.11	
Strain rate	<0.001*	Increasing	<0.05*	Trot>walk, gallop (rate magnitude)	<0.001*	Increasing	0.36		<0.0001*	Increasing	0.06	
Tr_{LAT}												
Strain	<0.0001*	Increasing lengthening	0.24		0.70		0.74		0.33		0.90	
Strain rate	<0.0001*	Increasing	0.25		<0.0001*	Increasing	0.60		0.72		0.822	
Kinematics												
Elbow angle Δ	<0.05*	Increasing flexion	0.24		<0.05*	Increasing extension	0.43		0.87		0.21	
Shoulder angle Δ	<0.01*	Increasing flexion	0.413		<0.0001*	Increasing extension	<0.001*	Trot, gallop>walk (extension magnitude)	<0.001*	Increasing extension	0.44	

These tests were conducted to estimate the effects of gait (d.f. 2) on muscle and limb function independently of speed (d.f. 1), as described in the text. These results are based on means at each speed for four individual goats, using the test as described in Table 1. Experimental data are given in Figs 4, 5 and 6. Differences among gaits were determined by Tukey's HSD tests performed *post hoc*.

*Statistically significant values.

†This result appears to be driven by a single individual (P<0.0001 for individual × speed during this period in a separate ANOVA, Table 1). Also see Fig. 5C.

throughout all phases of stance in all individuals at all speeds (Fig. 2, Fig. 5C).

Significant differences in fascicle strain magnitude were found between the two muscles during the yield phase as well as over total stance regardless of speed or gait (Figs 2 and 5). During the yield phase of stance the Tr_{LONG} shortened (–6.2±1.2%) and the Tr_{LAT} stretched (6.8±0.6%; P<0.001). No differences in strain magnitude were found during the propulsive phase when both muscles shortened (Tr_{LONG} –10.2±2.0% and Tr_{LAT} –10.6±2.7%, P>0.50; when grouped for all speeds and gaits). As a result, net shortening strain of the Tr_{LONG} (–16.4±3.4%) exceeded that of the Tr_{LAT} (3.5±2.4%; P<0.001) over total stance duration.

Paralleling the increase in elbow flexion with speed described in the previous section, the magnitude of Tr_{LAT} lengthening increased with speed (P<0.001), ranging from 4.7±1.1% at a 1.5 m s^{-1} walk to 8.7±1.8% at a 4 m s^{-1} trot (pooled mean ± s.e.m. of individual means at each speed, N=4). ANCOVA revealed a significant effect of individual (P<0.001; see Table 1 for test description), indicating that individual recordings of the Tr_{LAT} varied in their amount of shortening during the propulsive phase of stance (Fig. 5B). No independent effects of gait on Tr_{LAT} strain were observed (Table 2).

In the Tr_{LONG} the magnitude of shortening strain in the yield phase increased with increasing speed (P<0.001) ranging from –2.5±0.6%

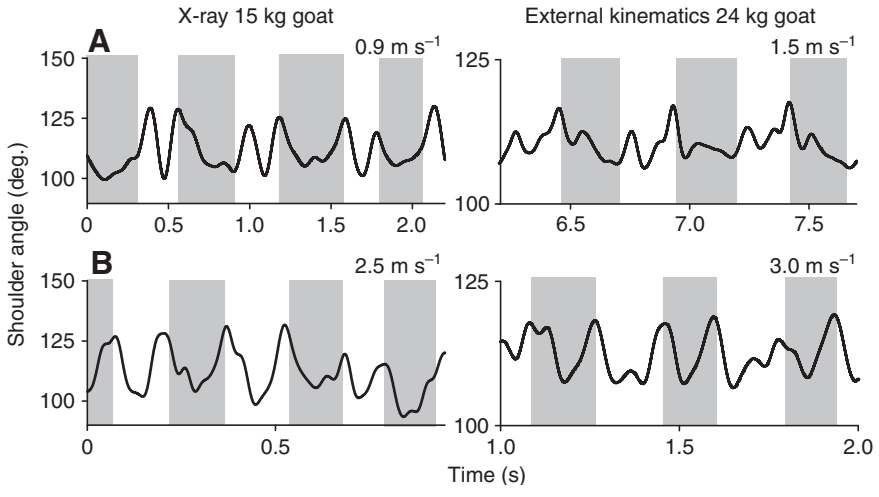

Fig. 3. Comparison of shoulder kinematics measured by X-ray video imaging (left) and external kinematics (right) during walk (A) and trot (B). The bold line is shoulder angle; the gray shading indicates estimated stance time as described in Materials and methods. (Sample videos are provided as supplementary material: Movies 1 and 2.) Overall, the patterns of flexion and extension were similar regardless of imaging technique, although shoulder angle magnitudes were greater in X-ray footage. This discrepancy may be due to differences in joint center estimation between external and internal kinematics.

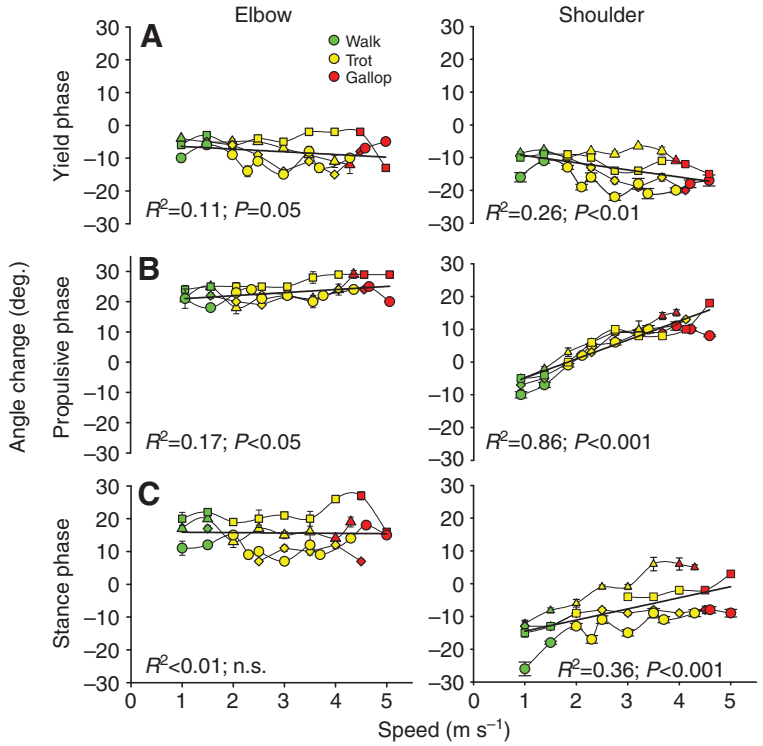

Fig. 4. Effect of speed (m s^{-1}) on angle change in the elbow (left) and shoulder (right), (A) in yield phase, (B) in propulsive phase and (C) over stance phase. Walks are in green, trots in yellow and gallops in red. Increases in speed caused increases in elbow flexion and extension magnitudes but net-stance angular excursion did not change with speed in the elbow. Likewise, shoulder flexion increased with speed as did extension (which was highly significant and shifted net flexion to net extension). Net-stance shoulder extension increased with speed, contributing to effective stride length.

at a 1.5 m s^{-1} walk to –6.5±2.7% at a 4 m s^{-1} trot. Yield phase Tr_{LONG} shortening also was influenced by gait, with greater shortening at a trot (–7.2±0.5%) than at a walk (–4.9±1%) or gallop (–2.3±0.9%; P<0.01; Table 2: values are least squares means ± s.e.m. from sequential ANCOVA as described in Table 1). The magnitude of shortening strain during the subsequent propulsive phase, however, decreased with increasing speed (P<0.05), ranging from –12.2±1.7% at a 1.5-m s^{-1} walk to –5.8±0.6% at a 4-m s^{-1} trot with no residual effect of gait (Table 2). The decreased magnitude of Tr_{LONG} shortening during the propulsive phase of stance with speed reflects the concurrent increase in shoulder extension (Fig. 4A).

No effect of speed on total stance phase Tr_{LONG} strain was observed (Table 2). However, this result appears to be driven by a single individual (Fig. 5C; speed×individual interaction P<0.001). Based on ANCOVA tests run within individual data sets (Table 1), three of the four individuals showed significant *increases* in shortening strain magnitude with speed (P<0.05, P<0.01, and P<0.0001, respectively), whereas one individual (squares in Fig. 5C)

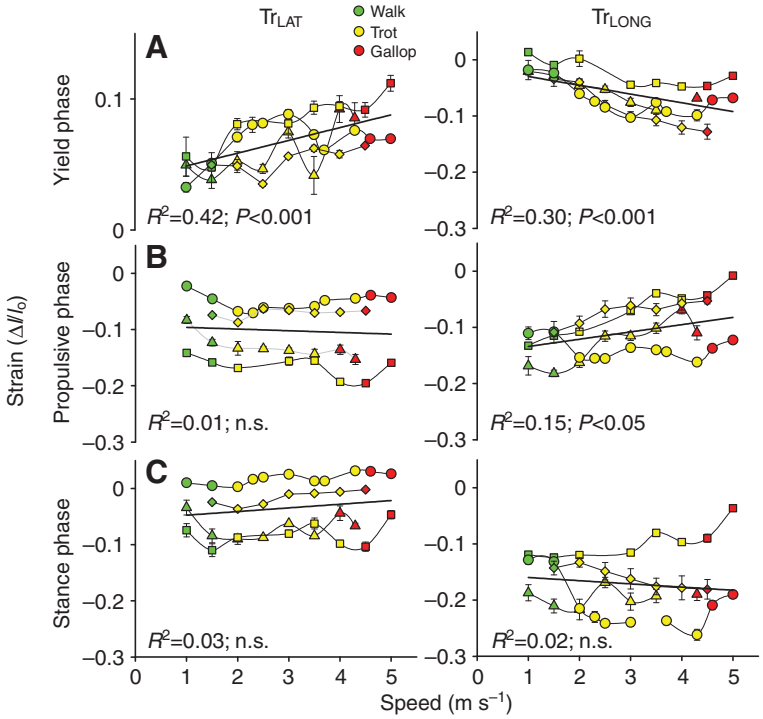

Fig. 5. Effect of speed (m s^{-1}) on fascicle strain ($\Delta l/l_o$) of the Tr_{LAT} (left) and Tr_{LONG} (right), (A) in yield phase, (B) in propulsive phase and (C) over stance phase. Walks are in green, trots in yellow and gallops in red. Each individual is denoted by a different symbol; values are means and s.e.m. Regression lines, r^2 values and P values are fitted to the entire data set, and P values for speed as a covariate for all gaits are given in Table 2. Stretch magnitude in the Tr_{LAT} increased with speed but no other trends were found among individuals. Shortening magnitude in the Tr_{LONG} increased with speed during yield phase and decreased with speed during propulsive phase. Over stance phase three individuals showed significant (P<0.05) increases in shortening magnitude, whereas one individual showed significant (P<0.05) decreases.

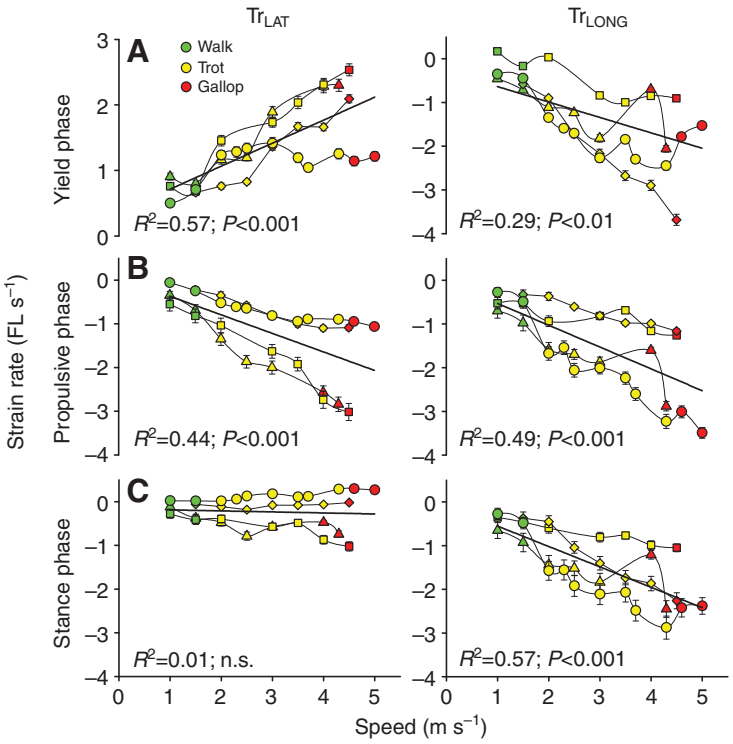

Fig. 6. Effect of speed ($m\,s^{-1}$) on fascicle strain rate (fascicle lengths s^{-1}) of the Tr_{LAT} (left) and Tr_{LONG} (right) in (A) yield phase, (B) propulsive phase and (C) over stance phase. Walks are in green, trots in yellow and gallops in red. Each individual is denoted by a different symbol; values are means and s.e.m. Regression lines, r^2 values, and P values are fitted to the entire data set, and P-values for speed as a covariate for all gaits are given in Table 2. Rate of stretch increased in the Tr_{LAT} for yield phase as did shortening for stance phase, but no increases in rate were detected over net stance. Strain rate increased in all phases of stance for the Tr_{LONG}.

exhibited a significant *decrease* in strain magnitude with speed (P<0.05).

Strain rate

When all speeds and gates were grouped, strain rates differed between the Tr_{LONG} and Tr_{LAT} in the yield phase [–1.41±0.30 *vs* 1.46±0.24 fascicle lengths per second ($FL\,s^{-1}$), respectively; P<0.001], and over stance (–1.39±0.23 *vs* –0.27±0.19 $FL\,s^{-1}$, respectively; P<0.001; Fig. 5). However, strain rates did not differ during the propulsive phase (–1.39±0.29 *vs* –1.30±0.31, respectively; P>0.05) when both muscle shortened (Fig. 5).

Fascicle strain rate patterns in the Tr_{LAT} resembled the patterns for strain magnitude, although strain rate regressions were more strongly correlated with speed (Fig. 6). Strain rates of Tr_{LAT} fascicles during the stance yield phase ranged from 0.73±0.02 $FL\,s^{-1}$ at 1.5 $m\,s^{-1}$ to 2±0.8 $FL\,s^{-1}$ at 4 $m\,s^{-1}$, and during the propulsive phase from –0.52±0.1 $FL\,s^{-1}$ at 1.5 $m\,s^{-1}$ to –2.1±0.5 $FL\,s^{-1}$ at 4 $m\,s^{-1}$. No effect of speed on Tr_{LAT} net shortening strain rate during stance was observed (P>0.50). Fascicle strain rates of the Tr_{LONG} increased with speed during yield, propulsive, and overall stance phases (despite reduced shortening strain with speed in the propulsive phase; Fig. 5B). Tr_{LONG} strain rates ranged from –0.55±0.15 $FL\,s^{-1}$ to –1.5±0.8 $FL\,s^{-1}$ in the yield phase, –0.7±0.23 $FL\,s^{-1}$ to –1.3±0.1 $FL\,s^{-1}$ in the propulsive phase, and –0.6±0.1 $FL\,s^{-1}$ to –1.4±03 $FL\,s^{-1}$ over stance, when compared at a 1.5 $m\,s^{-1}$ walk *versus* a 4 $m\,s^{-1}$ trot (Fig. 6).

Muscle activation

Both muscles were active for a portion of stance in all individuals and at all speeds. There was a small period of activation prior to limb reversal during the swing phase (Fig. 2), but the major period of activation in both muscles began before foot contact with the ground and ended before foot-off in both muscles (Fig. 2, Fig. 7A). EMG amplitude increased significantly with speed in both muscles (P<0.001) but showed no independent effects of gait. EMG onset occurred significantly earlier in the long head (64±5 ms before foot-on; –53±7% stance) than in the lateral head (33±5 ms before foot-on; –25±3% of stance; Fig. 7). No effect of speed on the absolute timing of EMG activation for either muscle was observed (P>0.20). As a percentage of stance, therefore, EMG onset time decreased with increasing speed (P<0.01 for both muscles, Table 3) as a result of decreased stance duration with speed. Consistent with its earlier activation onset, Tr_{LONG} activation also ended before that of the Tr_{LAT}. No effect of speed on activation offset of the Tr_{LONG} was observed in absolute (P>0.25) or relative stance time (P>0.10), with the mean offset time occurring 51±9 ms after foot-on, or 36±7% of

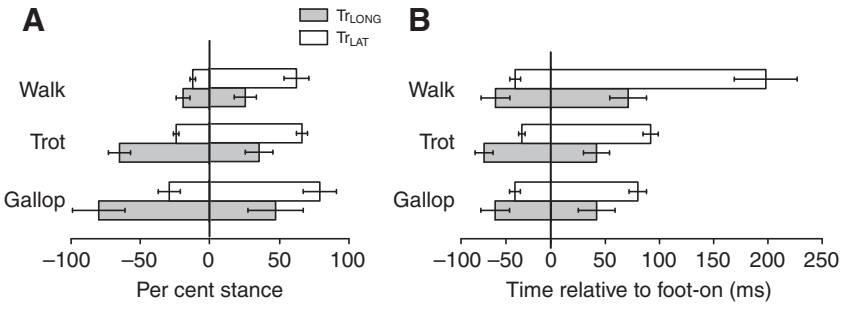

Fig. 7. Relative (A) and absolute (B) timing of muscle activation in the Tr_{LONG} and Tr_{LAT}. Bars denote duration of activity for the Tr_{LAT} (white) and Tr_{LONG} (gray) with s.e.m. Durations are expressed as a percentage of stance (A) and in absolute terms (B). Earlier onset times in the Tr_{LONG} may indicate a role in limb reversal at the end of swing phase. Overall trends in relation to speed and gait are discussed in the text, also see Table 3.

Table 3. *P*-values and trends from sequential (Type 1) ANOVA (d.f. in Table 1) results for speed and gait

	Speed		Gait	
	P value	Trend	*P*-value	Trend
Tr_{LONG}				
Onset (ms)	0.96		0.68	
Onset (% of stance)	<0.01*	Increasing relative onset	0.46	
Offset (ms)	0.28		0.72	
Offset (% of stance)	0.23		0.98	
EMG amplitude	<0.0001*	Increasing	0.17	
EMG duty factor	<0.0001*	Increasing	0.05*	Trot, gallop>walk
Tr_{LAT}				
Onset (ms)	0.16		0.70	
Onset (% of stance)	<0.01*	Decreasing relative offset	0.70	
Offset (ms)	<0.0001*	Decreasing	0.03*	Trot<gallop, walk
Offset (% of stance)	0.25		0.56	
EMG amplitude	<0.0001*	Increasing	0.65	
EMG duty factor	<0.0001*	Increasing	0.35	

Differences among gait types were determined by Tukey's HSD tests performed *post hoc*.
*Statistically significant values.

stance. EMG offset in the Tr_{LAT} occurred significantly (P<0.001) earlier after stance onset as speed increased, maintaining a constant (i.e. no effect of speed, P>0.25) activation offset at 68±6% stance. Although both muscles showed an increased activation duty factor with increasing speed (P<0.0001), the increase was greater for the Tr_{LONG} (Fig. 8), reflecting the conserved relative activation offset of the Tr_{LAT}. A significant independent effect of gait on Tr_{LONG} was also observed, with running gaits having a longer Tr_{LONG} EMG duty factor than walking, but this was not the case for Tr_{LAT} (Table 2).

DISCUSSION

We compared functional patterns in the long (Tr_{LONG}) and lateral (Tr_{LAT}) heads of the tricep brachii over a range of locomotor speeds and gaits in goats with the goal of understanding how differences in mono- *versus* biarticular anatomical organization lead to differences in functional pattern. Previously, we compared their roles during jumping take-off and landing (Carroll et al., 2008). Strain patterns differed markedly between the Tr_{LAT} and Tr_{LONG}, similar to differences observed during jumping. Whereas the Tr_{LAT} displayed a biphasic pattern of active stretch followed by active shortening during stance, the Tr_{LONG} actively shortened continuously throughout stance (Fig. 2). As hypothesized, a key difference between these patterns was the independence of the Tr_{LONG} from patterns of elbow flexion and extension made possible by of its biarticular organization. Specifically, flexion and extension patterns at the shoulder offset those at the elbow, allowing the Tr_{LONG} muscle to shorten during both the yield and propulsive phases of stance (Fig. 2). By contrast, the monoarticular Tr_{LAT} showed patterns of stretching during the yield phase of stance, and shortening during the propulsive phase that closely mirrored flexion and extension patterns of the elbow (Fig. 2).

Increases in speed were associated with increased fascicle strain magnitudes in both muscles, with increased stretch occurring during the yield phase and increased shortening during the propulsive phase in the Tr_{LAT}. Increased shortening in the Tr_{LONG} occurred during both phases (in three of the four individuals; Fig. 5, Table 2). Fascicle strain rates in both muscles also increased with increasing speed (Fig. 6), as did EMG intensity and EMG duty factor (Fig. 8). Few independent effects of gait on strain patterns were found when using a sequential (Type I) ANCOVA (Table 2). This finding supports the view that, although gait changes involve mechanically important changes in relative limb phase, limb muscle and joint patterns can largely be explained by changes in speed, rather than gait change,

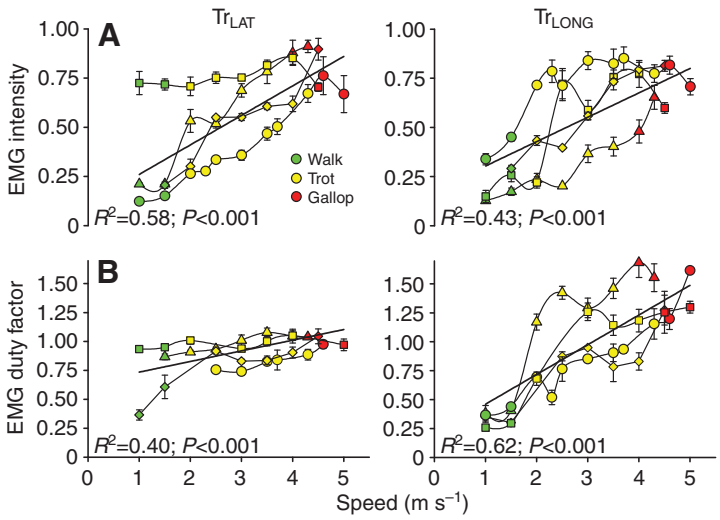

Fig. 8. Effect of speed (m s^{-1}) on normalized EMG amplitude and duty factor (normalized to stance time) in the Tr_{LAT} (left) and Tr_{LONG} (right). Walks are in green, trots in yellow, and gallops in red. Each individual is denoted by a different symbol; values are means and s.e.m. Regression lines, r^2 values, and P values are fitted to the entire data set, and P values for speed as a covariate for all gaits are given in Table 2. Both amplitude and duty factor increased with speed in both muscles; however, duty factor increased more precipitously in the Tr_{LONG}. Additional results are discussed in the text; also see Table 3.

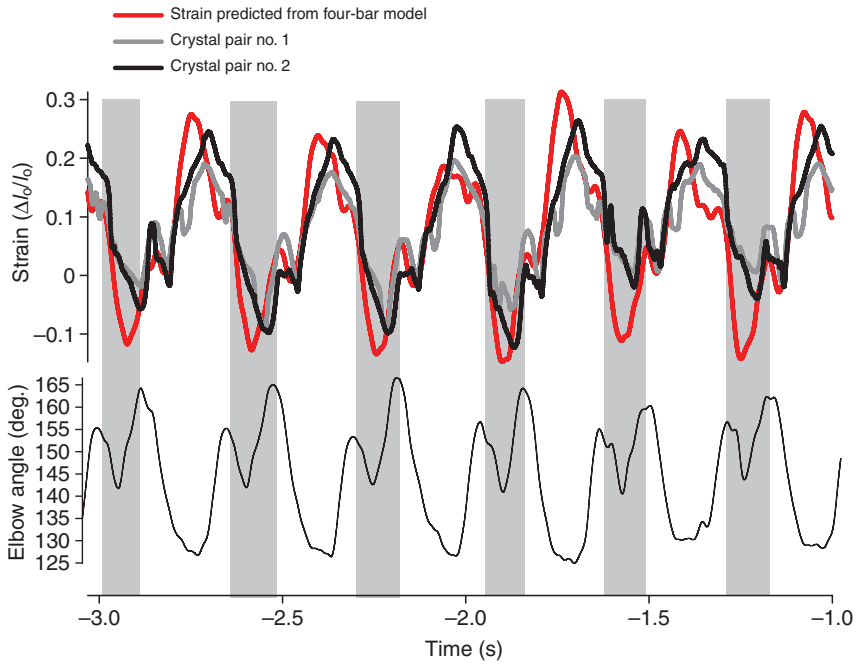

Fig. 9. Comparison of measured Tr_{LONG} strain (from two crystal pairs) *versus* that predicted from a four-bar linkage model in a 27 kg goat trotting at 3.5 m s^{-1}. The four bar linkage model is defined by the following equation:

$$\text{Predicted} = \sqrt{(\cos(\theta)\cdot l_s - (l_h - \cos(180-\lambda)\cdot l_{ol}))^2 + (\sin(\theta)\cdot l_s + \sin(180-\lambda)\cdot l_{ol})^2}\,,$$

where θ is the shoulder angle (deg.), λ is the elbow angle, and l_s, l_h and l_{ol} are the lengths of the scapula, humerus and olecranon process, respectively, of this individual. Notice that although there are differences between the measured and predicted traces (possibly because of series elasticity or scapular translation) the overall patterns are quite similar.

as previously noted by Fischer and Blickhan (Fischer and Blickhan, 2006).

Forelimb kinematics

In trots and gallops, stance began with elbow and shoulder flexion during the yield phase followed by re-extension during the propulsive phase (Fig. 2). This basic forelimb kinematic pattern has been observed in numerous small mammals (Fischer and Blickhan, 2006), cats (English, 1978) and dogs (Goslow et al., 1981). However, these studies found relatively little shoulder extension during the propulsive phase of stance. By contrast, we found that shoulder extension was of similar magnitude to flexion in goats during running gaits (Figs 2 and 4).

The magnitude of elbow flexion increased as speed increased (Fig. 4A). The increased flexion probably reflects an increased elbow moment, as contact time decreased and ground reaction forces probably increased, as has also been found in a variety of other animals (e.g. Biewener et al., 1983; Cavagna et al., 1977; Dutto et al., 2004; Kram and Taylor, 1990; Weyand et al., 2000). Elbow extension also increased with speed, compensating previous joint flexion to conserve net-stance elbow extension magnitude (Fig. 4). Likewise, both shoulder flexion and extension increased with speed. Increases in shoulder extension during the second phase of stance were, by far, the most consistent and significant relationships between speed and kinematics found in this study (Fig. 4B) and resulted in increased stride length. Increased stride length with speed has also appeared to result from increased shoulder extension and excursion in horses (Hudson-Tole, 2006), dogs (F. Jenkins, personal communication) and other mammals (Lilje et al., 2003). Thus, it appears that the elbow functions to compensate for the increased loading that results from decreased forelimb stance time as an animal's speed increases. By contrast, the shoulder functions to extend the leg, increasing stride length to help increase speed.

Muscle activation patterns

Consistent with our findings for the goat Tr_{LAT} and Tr_{LONG}, other studies examining motor activation patterns in one or both heads of the triceps [horses (Hudson-Tole, 2006; Tokuriki et al., 1989); dogs (Goslow et al., 1981); cats (English, 1978); and rats (Scholle et al., 2001)] have found these muscles to be active during stance. Increased EMG intensity at higher speeds has also been found in both heads of the horse triceps (Hoyt et al., 2005; Hudson-Tole, 2006) and is probably a response to increased joint and muscle loading. Similar increases in intensity have been found in the vastus lateralis and biceps femoris of goats (Gillis et al., 2005) and rats (Gillis and Biewener, 2001).

We also observed a brief period of Tr_{LONG} activity at the end of swing during faster trotting and galloping speeds, which fused with the stance phase activation of the muscle (Fig. 2C), as has been found in dogs (Tokuriki et al., 1989). Thus, it is possible that active Tr_{LONG} triceps force generation is required for limb reversal at the end of swing at higher speeds. The absolute delay between Tr_{LAT} activation and foot down found in this study (~33 ms) was similar to that found in the Tr_{LAT} of horses by Hoyt et al. (Hoyt et al., 2005), who also found this to be invariant with speed. This pattern probably reflects excitation–contraction delays in muscle force development (Lieber, 2002) required to anticipate limb and elbow joint loading. The Tr_{LONG} tended to be activated and deactivated before the Tr_{LAT} in

absolute terms, as well as a percentage of stance duration, perhaps reflecting a reduction in required shoulder moments near the end of stance.

Comparison of muscle strain patterns

As we hypothesized, the monoarticular Tr_{LAT} stretched and shortened in close association with the flexion–extension patterns of the elbow joint, consistent with earlier predictions from kinematics and EMG recordings of the dog lateral triceps (Goslow et al., 1981). Surprisingly, the contractile pattern differed from that found in the horse Tr_{LAT}, which showed minimal (~2%) lengthening during trotting (Hoyt et al., 2005), despite a similar magnitude of elbow flexion (~5 deg.). More broadly, the stretch-shortening strain pattern in the Tr_{LAT} resembled patterns observed *in vivo* in the monoarticular VL of goats (Gillis et al., 2005), rats (Gillis and Biewener, 2001) and humans (Ishikawa et al., 2005b), associated with knee flexion and extension during stance. The stretch-shortening strain pattern of the Tr_{LAT} was also similar to the contractile patterns of the muscle in take-off and landing during jumping (Carroll et al., 2008).

Based on X-ray ciné, the Tr_{LONG} has been predicted to shorten throughout stance in running dogs (Goslow et al., 1981), but sonomicrometric recordings from the dog Tr_{LONG} have only shown shortening during the yield phase (Gregersen et al., 1998). By contrast, we found continuous shortening in the Tr_{LONG} during the entirety of stance across both speed and gait changes, similar to its pattern during jump take-offs when overall limb and joint work must be generated (Carroll et al., 2008). The Tr_{LONG} shortened initially as a result of shoulder flexion (offsetting its tendency to stretch because of concurrent elbow flexion), then continued to shorten because of subsequent elbow extension during the latter half of stance. This pattern of continuous shortening has also been measured in the biarticular semimembranosus of trotting dogs (Gregersen et al., 1998), but generally has not been predicted for biarticular muscles (e.g. van Ingen Schenau, 1990; Fischer and Blickhan, 2006).

We interpret differences in strain patterns between the Tr_{LONG} and Tr_{LAT} largely in terms of differences in the anatomical organization of the muscles. However, other differences between the two muscle heads, such as Tr_{LONG} pinnation, may also contribute to these differences. To evaluate this possibility, strain patterns in the Tr_{LONG} were compared with those predicted using a four-bar linkage model (Figs 8 and 9) and found to be qualitatively similar. A similar difference based on ultrasound visualization was found between the biarticular medial gastrocnemius (MG) and monoarticular soleus of humans (Loram et al., 2006), with the soleus following ankle joint kinematics more closely than the MG. By contrast, estimation of strain patterns based on joint kinematics have shown similar patterns between the monoarticular and biarticular muscles of the triceps surae of cats (e.g. Prilutsky et al., 1996). We consider that this difference arises because of the difficulty of assessing accurately the series elastic compliance of muscle–tendon units when estimating muscle strain patterns from joint kinematics.

van Ingen Schenau (van Ingen Schenau, 1990) posited that monoarticular muscles are mainly activated to produce force to contribute positive work, whereas biarticular muscles are activated to distribute net joint moments to control the direction of force applied externally by the limb. The differences in strain pattern we observed between the Tr_{LAT} and the Tr_{LONG}, however, appear inconsistent with this functional distinction. The Tr_{LONG} actively shortened throughout stance (–16.4±3.4% mean over all speeds and gaits), indicating positive work production, whereas the Tr_{LAT} underwent alternate active lengthening and shortening, suggesting energy absorption followed by production (Fig. 3). Thus, the biarticular Tr_{LONG} appears to function to produce work throughout stance, similar to its role during jump take-offs (Carroll et al., 2008). Furthermore, its size and architecture (relatively massive, long-fibered) are consistent with this function. Rather than being limited to the distribution of joint moments and energy transfer, the biarticular anatomy of the Tr_{LONG} allows it to shorten throughout stance, probably contributing significant work, in addition to any energy that it may additionally transfer across these two joints of the proximal forelimb. By comparison, the Tr_{LAT} appears to produce work only in the propulsive phase of stance, after absorbing energy at the elbow during the yield phase, tracking the flexion–extension dynamics of the elbow joint. It should be noted that these inferences are based on strain and EMG patterns alone and not direct measurements of muscle force and work production, and, thus, should be treated with some caution.

In contrast to the shortening observed in the biarticular goat Tr_{LONG}, hind limb biarticular muscles in running turkeys (Roberts et al., 1997) and guinea fowl (Daley and Biewener, 2003), hopping wallabies (Biewener et al., 1998) and walking and running humans (Ishikawa et al., 2005a; Lichtwark et al., 2007) display nearly isometric muscle function. Consequently, differences in their contractile behavior probably reflect other anatomical differences. First, whereas the Tr_{LONG} has a long moment arm at the shoulder relative to its moment arm at the elbow (Fig. 1), the proximal moment arms of the hind limb lateral and medial gastrocnemius at the knee are small relative to the muscles' moment arm at the ankle, reducing the influence of the knee joint on LG and MG length change behavior (Kaya et al., 2005). Second, fascicle length changes of the LG and MG are buffered from ankle joint kinematics by their comparatively long compliant tendon (Lichtwark and Wilson, 2006). By contrast, the tendon attachment of Tr_{LONG} at the elbow is extremely short, so that Tr_{LONG} fascicle length changes are more closely coupled to joint kinematics. Indeed, the monoarticular Tr_{LAT} stretch-shorten strain pattern is much more similar to that of the biarticular LG and MG muscles, despite the magnitudes of lengthening and shortening in the Tr_{LAT} being greater because of the absence of a compliant tendon. The similarities in strain patterns suggest that energy absorption at the elbow during the yield phases of stance is important, as is energy absorption at the ankle. The greater magnitude of fascicle strain in the Tr_{LAT} suggests that energy absorption is accomplished mainly by the muscle fascicles.

Effect of speed on muscle function

By examining the effect of speed on muscle strain patterns, it is possible to consider how speed-related changes may affect changes in the metabolic cost of locomotion (Heglund et al., 1982; Taylor, 1994; Roberts et al., 1998; Hedrick et al., 2003) and may, therefore, limit an animal's top sustainable speed. In both the goat Tr_{LONG} and Tr_{LAT} EMG intensity increased with speed, suggesting an increase in recruited muscle volume and the possibility of concurrent increases in the metabolic cost of locomotion. Such increases in recruited muscle volume are expected and have been observed in other studies as well (Daley and Biewener, 2003; Gillis and Biewener, 2001). An increase in recruited muscle volume, with little change in contractile strain behavior, is consistent with increased muscle force production being the primary determinant of an increase in rate of metabolic energy use associated with speed (Kram and Taylor, 1990). In certain muscles examined to date, the magnitude of shortening strain appears not to increase substantially with speed (Hoyt et al., 2005; Gillis et al., 2005; Roberts et al., 2007), supporting a pattern of changes in muscle recruitment and

force being the major determinant of metabolic cost. In the present study, however, net contractile strains in the Tr_{LONG} increased with speed (Fig. 5), and such increases have also been observed in the Tr_{LONG} of dogs (Gregersen et al., 1998) and in the LG of guinea fowl (Daley and Biewener, 2003). Such increases in active shortening strain probably increase the work done by a muscle above that predicted by volume recruitment alone, contributing to an additional increase in the cost of locomotion. As a result, increases in muscle force and work output probably play a role in limiting the maximum sustained speed of an animal. The biarticular arrangement of the Tr_{LONG} may help mitigate the effects of speed on strain magnitude by allowing shoulder and elbow joint motions to offset their effect on the muscle's overall length change. Shoulder extension in the propulsive phase of stance increased with speed (Fig. 4), probably reducing speed-related effects on increased Tr_{LONG} shortening and work output, and thus, the muscle's contribution to increases in overall metabolic energy use rate.

Conclusions

Differences in anatomical configuration between the biarticular Tr_{LONG} and monoarticular Tr_{LAT} of goats appear to underlie significant differences in strain patterns displayed by each muscle during steady level locomotion. Whereas the monoarticular Tr_{LAT} stretched and shortened during the yield and propulsive phases of stance in a pattern that closely mirrored flexion-extension of the elbow, the biarticular Tr_{LONG} shortened throughout stance. This was mediated by shoulder flexion during the yield phase, and a combination of shoulder extension that exceeded elbow extension during the propulsive phase. The apparent functional role of the goat Tr_{LONG} for work production during steady speed locomotion is in contrast to the commonly predicted role of biarticular muscles: to distribute moments across adjacent joints and transfer energy but to contribute little or no work. This latter behavior of biarticular muscles has been observed in hind limb triceps surae leg muscles, in which the nearly isometric contractile behavior is facilitated by transmitting force *via* long compliant tendons. By contrast, both the biarticular Tr_{LONG} and monoarticular Tr_{LAT} lack a compliant distal tendon attachment at the elbow. As a result, length changes of both these muscles are largely accommodated by the muscle's fascicles and not by the muscle's series elastic structures. As speed increased, the Tr_{LONG} showed increases in strain (in most individuals) and strain rate (Figs 5 and 6), and the Tr_{LAT} showed increases in stretching strain and stretch and shortening strain rate (Figs 5 and 6). These changes in muscle strain pattern, along with increases in muscle recruitment suggested by increased EMG intensity with speed, probably underlie an increased metabolic cost of muscle usage, contributing to an increased cost of locomotion and limiting the maximum sustainable speed of goats.

Pedro Ramirez maintained and helped to train the goats used in this study, and was invaluable in facilitating this research. Carlos Moreno, Russell Main, Craig McGowan, Edwin Yoo, Ivo Ros, Kieth Egan, Cathy Handy, Emily Niu and Trevor Higgins assisted in data collection. Craig McGowan also donated his inverse dynamics script. This research was supported by NIH grant AR-047679 to A.A.B. Deposited in PMC for release after 12 months.

REFERENCES

Biewener, A. A., Thomason, J. J. and Lanyon, L. E. (1983). Mechanics of locomotion and jumping in the forelimb of the horse (*Equus*): *in vivo* stresses developed in the radius and metacarpus. *J. Zool. Lond.* **201**, 67-82.

Biewener, A. A. and Roberts, T. J. (2000). Muscle and tendon contributions to force, work, and elastic energy savings: a comparative perspective. *Exerc. Sport Sci. Rev.* **28**, 99-107.

Biewener, A. A., Konieczynski, D. D. and Baudinette, R. V. (1998). *In vivo* muscle force-length behavior during steady-speed hopping in tammar wallabies. *J. Exp. Biol.* **201**, 1681-1694.

Carroll, A. M., Lee, D. V. and Biewener, A. A. (2008). Differential muscle function between muscle synergists: long and lateral heads of the triceps in jumping and landing goats (*Capra hircus*). *J. Appl. Physiol.* **105**, 1262-1273.

Cavagna, G. A., Heglund, N. C. and Taylor, C. R. (1977). Mechanical work in terrestrial locomotion: two basic mechanisms for minimizing energy expenditure. *Am. J. Physiol.* **233**, R243-R261.

Cleland, J. (1867). On the actions of muscles passing over more than one joint. *J. Anat. Physiol.* **1**, 85-93.

Daley, M. A. and Biewener, A. A. (2003). Muscle force-length dynamics during level *versus* incline locomotion: a comparison of *in vivo* performance of two guinea fowl ankle extensors. *J. Exp. Biol.* **206**, 2941-2958.

Dutto, D. J., Hoyt, D. F., Cogger, E. A. and Wickler, S. J. (2004). Ground reaction forces in horses trotting up an incline and on the level over a range of speeds. *J. Exp. Biol.* **207**, 3507-3514.

English, A. W. (1978). An electromyographic analysis of forelimb muscles during overground stepping in the cat. *J. Exp. Biol.* **76**, 105-122.

Fischer, M. S. and Blickhan, R. (2006). The tri-segmented limbs of therian mammals: kinematics, dynamics, and self-stabilization: a review. *J. Exp. Zool. A Comp. Exp. Biol.* **305**, 935-952.

Gillis, G. B. and Biewener, A. A. (2001). Hindlimb muscle function in relation to speed and gait: *in vivo* patterns of strain and activation in a hip and knee extensor of the rat (*Rattus norvegicus*). *J. Exp. Biol.* **204**, 2717-2731.

Gillis, G. B., Flynn, J. P., McGuigan, P. and Biewener, A. A. (2005). Patterns of strain and activation in the thigh muscles of goats across gaits during level locomotion. *J. Exp. Biol.* **208**, 4599-4611.

Gorb, S. V. and Fischer, M. S. (2000). Three-dimensional analysis of the arrangement and length distribution of fascicles in the triceps muscle of *Galea musteloides* (Rodentia, Cavimorpha). *Zoomorphology* **120**, 91-97.

Goslow, G. E., Jr, Seeherman, H. J., Taylor, C. R., McCutchin, M. N. and Heglund, N. C. (1981). Electrical activity and relative length changes of dog limb muscles as a function of speed and gait. *J. Exp. Biol.* **94**, 15-42.

Gregersen, C. S., Silverton, N. A. and Carrier, D. R. (1998). External work and potential for elastic storage at the limb joints of running dogs. *J. Exp. Biol.* **201**, 3197-3210.

Hedrick, T. L., Tobalske, B. W. and Biewener, A. A. (2003). How cockatiels (*Nymphicus hollandicus*) modulate pectoralis power output across flight speeds. *J. Exp. Biol.* **206**, 1363-1378.

Heglund, N. C., Fedak, M. A., Taylor, C. R. and Cavagna, G. A. (1982). Energetics and mechanics of terrestrial locomotion. IV. Total mechanical energy changes as a function of speed and body size in birds and mammals. *J. Exp. Biol.* **97**, 57-66.

Hoyt, D. F., Wickler, S. J., Biewener, A. A., Cogger, E. A. and De La Paz, K. L. (2005). *In vivo* muscle function *vs* speed. I. Muscle strain in relation to length change of the muscle-tendon unit. *J. Exp. Biol.* **208**, 1175-1190.

Hudson-Tole, E. (2006). Effects of treadmill inclination and speed on forelimb muscle activity and kinematics of the horse. *Equine Comp. Ex. Phys.* **3**, 61-72.

Ishikawa, M., Komi, P. V., Grey, M. J., Lepola, V. and Bruggemann, G. P. (2005a). Muscle-tendon interaction and elastic energy usage in human walking. *J. Appl. Physiol.* **99**, 603-608.

Ishikawa, M., Niemela, E. and Komi, P. V. (2005b). Interaction between fascicle and tendinous tissues in short-contact stretch-shortening cycle exercise with varying eccentric intensities. *J. Appl. Physiol.* **99**, 217-223.

Jacobs, R., Bobbert, M. F. and van Ingen Schenau, G. J. (1993). Function of mono- and biarticular muscles in running. *Med. Sci. Sports Exerc.* **25**, 1163-1173.

Kaya, M., Jinha, A., Leonard, T. R. and Herzog, W. (2005). Multi-functionality of the cat medical gastrocnemius during locomotion. *J. Biomech.* **38**, 1291-1301.

Kram, R. and Taylor, C. R. (1990). Energetics of running: a new perspective. *Nature* **346**, 265-267.

Lichtwark, G. A. and Wilson, A. M. (2006). Interactions between the human gastrocnemius muscle and the Achilles tendon during incline, level and decline locomotion. *J. Exp. Biol.* **209**, 4379-4388.

Lichtwark, G. A., Bougoulias, K. and Wilson, A. M. (2007). Muscle fascicle and series elastic element length changes along the length of the human gastrocnemius during walking and running. *J. Biomech.* **40**, 157-164.

Lieber, R. L. (2002). *Skeletal Muscle Structure, Function and Plasticity: The Physiological Basis of Rehabilitation*. Philadelphia, PA: Lippincott Williams and Wilkins.

Lilje, K., Tardieu, C. and Fischer, M. S. (2003). Scaling of long bones in ruminants with respect to the scapula. *J. Zoolog. Syst. Evol. Res.* **41**, 118-126.

Loeb, G. E. and Gans, C. (1986). *Electromyography for Experimentalists*. Chicago, IL: University of Chicago Press.

Loram, I. D., Maganaris, C. N. and Lakie, M. (2006). Use of ultrasound to make noninvasive *in vivo* measurement of continuous changes in human muscle contractile length. *J. Appl. Physiol.* **100**, 1311-1323.

Marsh, R. L. and Ellerby, D. J. (2006). Partitioning locomotor energy use among and within muscles: muscle blood flow as a measure of muscle oxygen consumption. *J. Exp. Biol.* **209**, 2385-2394.

Mol, C. R. and Breddels, P. A. (1982). Ultrasound velocity in muscle. *J. Acoust. Soc. Am.* **71**, 455-461.

Payne, R. C., Hutchinson, J. R., Robilliard, J. J., Smith, N. C. and Wilson, A. M. (2005a). Functional specialisation of pelvic limb anatomy in horses (*Equus caballus*). *J. Anat.* **206**, 557-574.

Payne, R. C., Veenman, P. and Wilson, A. M. (2005b). The role of the extrinsic thoracic limb muscles in equine locomotion. *J. Anat.* **206**, 193-204.

Phillipson, M. (1905). L'autonomie et la centralization dans le systeme nerveux des animaux. *Travails du Laboratoire de la Physiologie, Institut Solvey* **7**, 1-208.

Prilutsky, B. I. and Zatsiorsky, V. M. (1994). Tendon action of two-joint muscles: transfer of mechanical energy between joints during jumping, landing, and running. *J. Biomech.* **27**, 25-34.

Prilutsky, B. I., Herzog, W. and Allinger, T. L. (1996). Mechanical power and work of cat soleus, gastrocnemius and plantaris muscles during locomotion: possible functional significance of muscle design and force patterns. *J. Exp. Biol.* **199**, 801-814.

Roberts, T. J., Marsh, R. L., Weyand, P. G. and Taylor, C. R. (1997). Muscular force in running turkeys: the economy of minimizing work. *Science* **275**, 1113-1115.

Roberts, T. J., Kram, R., Weyand, P. G. and Taylor, C. R. (1998). Energetics of bipedal running. I. Metabolic cost of generating force. *J. Exp. Biol.* **201**, 2745-2751.

Roberts, T. J., Higginson, B. K., Nelson, F. E. and Gabaldon, A. M. (2007). Muscle strain is modulated more with running slope than speed in wild turkey knee and hip extensors. *J. Exp. Biol.* **210**, 2510-2517.

Scholle, H. C., Schumann, N. P., Biedermann, F., Stegeman, D. F., Grassme, R., Roeleveld, K., Schilling, N. and Fischer, M. S. (2001). Spatiotemporal surface EMG characteristics from rat triceps brachii muscle during treadmill locomotion indicate selective recruitment of functionally distinct muscle regions. *Exp. Brain Res.* **138**, 26-36.

Taylor, C. R. (1994). Relating mechanics and energetics during exercise. In *Comparative Vertebrate Exercise Physiology* (ed. J. H. Jones), pp. 181-215. San Diego, CA: Academic Press.

Tokuriki, M., Aoki, O., Niki, Y., Kurakawa, Y., Hataya, M. and Kita, T. (1989). Electromyographic activity of cubital joint muscles in horses during locomotion. *Am. J. Vet. Res.* **50**, 950-957.

van Ingen Schenau, G. J. (1990). On the action of bi-articular muscles, a review. *Neth. J. Zool.* **40**, 521-540.

Weyand, P. G., Sternlight, D. B., Bellizzi, M. J. and Wright, S. (2000). Faster top running speeds are achieved with greater ground forces not more rapid leg movements. *J. Appl. Physiol.* **89**, 1991-1999.

Williams, S. B., Wilson, A. M., Rhodes, L., Andrews, J. and Payne, R. C. (2008). Functional anatomy and muscle moment arms of the pelvic limb of an elite sprinting athlete: the racing greyhound (*Canis familiaris*). *J. Anat.* **213**, 361-372.

Witte, H., Biltzinger, J., Hackert, R., Schilling, N., Schmidt, M., Reich, C. and Fischer, M. S. (2002). Torque patterns of the limbs of small therian mammals during locomotion on flat ground. *J. Exp. Biol.* **205**, 1339-1353.